Soils and Foundations 2012;52(4):634–643

The Japanese Geotechnical Society

Soils and Foundations

www.sciencedirect.com
journal homepage: www.elsevier.com/locate/sandf

Effect study of cracks on behavior of soil slope under rainfall conditions

Ga Zhang[a,b,*], Rui Wang[a], Jiyun Qian[a], Jian-Min Zhang[a], Jiangu Qian[b]

[a]State Key Laboratory of Hydroscience and Engineering, Tsinghua University, China
[b]Key Laboratory of Geotechnical and Underground Engineering of Ministry of Education, Tongji University, China

Received 28 October 2011; received in revised form 20 March 2012; accepted 1 May 2012
Available online 15 August 2012

Abstract

Deep-seated landslides in slopes are often induced by rainfall due to pre-existing cracks or weak layers. A series of centrifuge model tests under rainfall conditions were conducted on slopes with different types of cracks. The histories of suction and displacement of the slope were measured during the tests to investigate the infiltration–deformation–failure process of the slopes. The wetting front curved notably near the crack under rainfall conditions. The deformation of the slope was mainly caused by the saturation of soil and crack-affected water infiltration under rainfall conditions. The displacement process of the slopes with cracks can be divided into a small displacement stage, a rapid increase stage, and a stable stage. The influence of the crack on the infiltration and deformation of the slope decreased with increasing distance from the crack. Rainfall induced significant vertical deformation near the vertical crack rather than horizontal deformation. In contrast to the oblique crack, the vertical crack on the slope top was unlikely to lead to global landslide under rainfall conditions. The deformation–failure behavior of the slope with cracks was also affected by the rainfall style and rain intensity.

Keywords: Slope; Rainfall; Crack; Failure; Deformation; Infiltration; Centrifuge model test

1. Introduction

Rainfall is a major cause of slope failures that claim the lives of many and lead to significant economic losses around the world. Laboratory and field tests have indicated that a homogeneous slope under rainfall conditions is prone to suffer from surface erosion or shallow landslides (e.g., Yuki et al., 2006; Montrasio et al., 2009; Zhang et al., 2011), whereas surveys of landslides have demonstrated that deep-seated failures are often induced by rainfall in slopes with pre-existing cracks or weak layers (e.g., Hu, 2000; Fan et al., 2005; Wang et al., 2010b). For example, Rogers and Selby (1980) described landslides in New Zealand caused by pore pressures within cracks after rainstorms. It can be concluded that cracks have a significant effect on the rainfall-induced failure behavior of the slope. While the stability level of slopes with cracks should be reasonably evaluated under rainfall conditions, such an evaluation is dependent on a thorough understanding of the infiltration–deformation–failure response of such a slope. Unfortunately, the effect of cracks on these behaviors of soil slopes under rainfall conditions has yet to be systematically investigated.

*Correspondence to: Institute of Geotechnical Engineering, Department of Hydraulic Engineering, Tsinghua University, Beijing 100084, PR China. Tel./fax: +86 10 62795679.
E-mail addresses: zhangga@tsinghua.edu.cn (G. Zhang), wr05@mails.tsinghua.edu.cn (R. Wang), qianjiyun@gmail.com (J. Qian), zhangjm@tsinghua.edu.cn (J.-M. Zhang), qianjiangu@tongji.edu.cn (J. Qian).
Peer review under responsibility of The Japanese Geotechnical Society.

Production and hosting by Elsevier

0038-0806 © 2012 The Japanese Geotechnical Society. Production and hosting by Elsevier B.V. All rights reserved.
http://dx.doi.org/10.1016/j.sandf.2012.07.005

Table 1
List of centrifuge model tests for slopes with cracks.

No.	Rainfall style	Rain intensity (mm/min)	Crack style	Final rainfall amount
1♯	Common	2.5	Vertical	35 mm
2♯	Common	1.5	Vertical	40 mm
3♯	Common	1.0	Vertical	40 mm
4♯	Concentrated		Oblique	0.6 L
5♯	Concentrated		Vertical	1.8 L

Field observations and full-scale tests have been widely used to study the deformation response and failure modes of the slope under rainfall conditions. For example, it has been generally discovered that rain infiltration induced an evident reduction in the suction of the soil and the shear strength of the soil decreases accordingly, and that this preceded the rainfall-induced failure of soil slopes (e.g., Lim et al., 1996; Trandafir et al., 2008). A full-scale landslide test indicated that the rapid increase of rainfall-induced pore water pressure is critical to the initiation of the slope's failures (Moriwaki et al., 2004).

The rainfall-induced deformation of the slope, as well as the main influential factors, could be further analyzed using the finite element method or other numerical methods (e.g., Anderson and Pope, 1984; Iverson, 2000). The stability level of the slope under rainfall conditions was usually estimated using the limit equilibrium method (e.g., Zolfaghari et al., 2005); however, the reliability of such a method is significantly influenced by a few factors, such as a reasonable analysis of the infiltration field of the slope.

The model test is an important approach for investigating the behavior of a slope during rainfall because the processes of infiltration, deformation, and failure can be observed and measured with well-controlled boundary conditions (e.g., Wang and Sassa, 2001; Tohari et al., 2007). Centrifuge model tests have been widely employed in studies on the slopes under different conditions as similar stress levels of the prototype can be simulated in a small-scale model by increasing centrifugal acceleration (e.g., Take et al., 2004; Viswanadham and Rajesh, 2009; Wang et al., 2010a). A challenge of the rainfall centrifuge model test is to simulate rainfall with good uniformity and controlled intensity. A few researchers (e.g., Kimura et al., 1991; Take et al., 2004; Hudacsek et al., 2009) achieved the simulation of rainfall in centrifuge tests through arranging spray nozzles above the slope and investigated slope responses to both medium- and long-term rainfall events. Zhang et al. (2011) provided an alternative method for rainfall simulation in the centrifuge and conducted a series of centrifuge tests to analyze the deformation mechanism of homogeneous cohesive soil slopes.

Previous studies have placed the majority of their focus on homogeneous slopes under rainfall conditions. The deformation response and failure mechanism of the slope with pre-existing cracks under rainfall conditions have not been thoroughly clarified, though cracks are widely distributed in practical slopes and these have potential to accelerate the failure of the slopes. In this paper, a series of centrifuge model tests was conducted on slopes with different types of cracks under rainfall conditions. The histories of suction and displacement of the slope were measured during the tests. Thus, the effect of cracks on the rainfall-induced infiltration–deformation–failure of the slopes was analyzed according to the test observations.

2. Test models

2.1. Schemes

Table 1 lists the test schemes for the slope with cracks. Two types of cracks, vertical and oblique, were simulated in the tests to consider the effect of the crack types. The inclination of the oblique crack was chosen to be 42°, close to the inclination of the slope and significantly different from that of the vertical crack. The centrifuge model tests used two rainfall styles. One was a common rainfall with three different intensities that was realized through the rainfall simulator, and the other was concentrated infiltration through the crack of the slope. It should be noted that the concentrated infiltration case was chosen as an extreme case of increased rainfall infiltration at the crack to study the effect on slope deformation of water seeping through the crack. The centrifuge model tests were conducted at 50 g of centrifuge acceleration, and the prototype height of the slope was 15 m, which is considered a moderate size. In addition, the observation results of homogeneous slopes with the same slope geometry were used for possible comparisons with the slopes with cracks (Wang et al., 2010b).

2.2. Devices

The centrifuge model tests were conducted using the 50 g t geotechnical centrifuge of Tsinghua University with a maximum centrifugal acceleration of 250 g. The model container was 500 mm long, 200 mm wide, and 500 mm high.

A rainfall simulation system was used to realize uniform rainfall during the centrifuge model tests (Zhang et al., 2011). Rainfall is initiated and maintained through an air pressure system and dispersed as tiny raindrops through a layer of a low permeability textile with densely covered tiny pores. The rain intensity can be adjusted by changing the air pressure, and the evenness of the rainfall on the surface of the slope was assured with specially designed container sides and a wind-proof structure.

The concentrated infiltration was simulated using a pipe with tiny holes that was placed on the top of the filters in the crack of the slope. Water was stored in a water tank that was fixed on the radial beam of the centrifuge machine. A magnetic valve was set at the export of the water tank to control the flow. Water was driven by the centrifugal force from the tank to the crack through the pipe when the valve was switched on during the centrifuge model test.

2.3. Slope model

The cohesive soil of a subway station, with an average grain size of 0.03 mm and specific gravity of 2.71, was used for the slope model. The plastic limit and liquid limit of the soil are 15% and 28%, respectively. According to the standard proctor test, the maximum dry density and corresponding optimum water content are 1.803 g/cm^3 and 16%, respectively.

The soil was compacted to 6 cm-thick layers in the model container using an impact hammer, thereby obtaining a dry density of 1.5 g/cm^3 and an initial water content of 17.5%. The slope was 30 cm high with an inclination of 45° (Fig. 1). Fig. 2 shows a photo of a model slope with a vertical crack prior to spin up. A 6 cm high horizontal soil layer was maintained under the slope to eliminate the effect of the container on the slope. Silicone oil was painted on both sides of the container to decrease the slope-container friction.

The crack, in either a vertical direction or an oblique direction, was preset in the slope when the sample was prepared by pre-laying a thin rigid metal sheet during the construction of the slope. A few pieces of common quantitative fine filter paper sheets were inserted into the crack as the metal sheet was taken out upon completion of the slope to avoid the possible closure of the crack. The post-test observations showed that the filter paper can hold

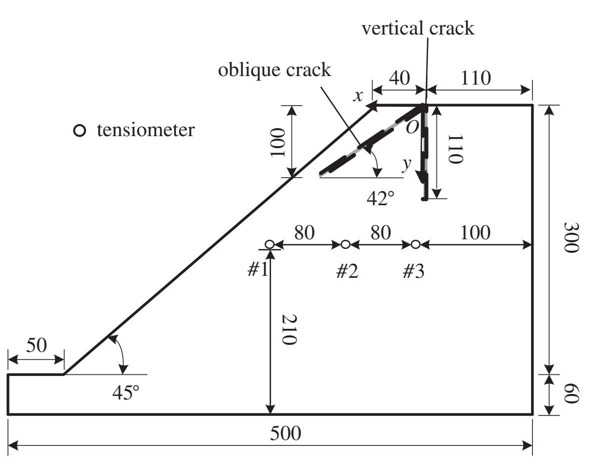

Fig. 1. Schematic view of the slope model (mm).

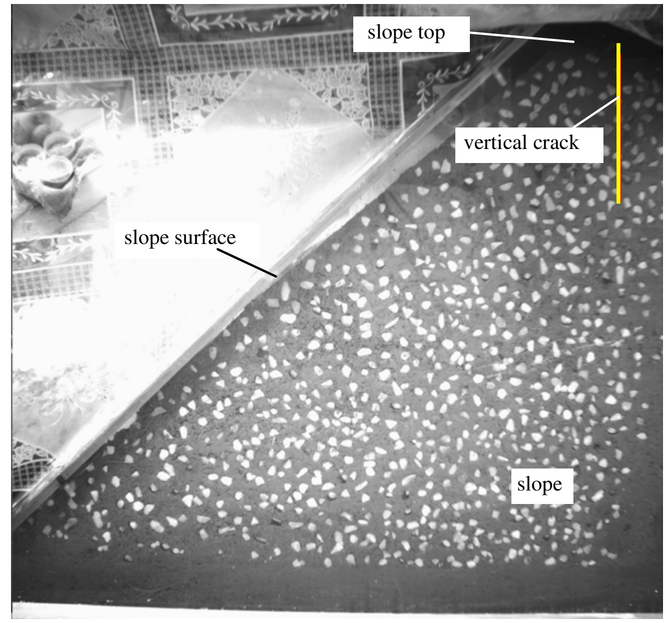

Fig. 2. Photograph of a typical slope model.

the crack during the centrifuge model tests. The crack was approximately 1 mm in thickness. The vertical and oblique cracks were 110 mm and 100 mm in depth, equivalent to 550 mm and 500 mm in the prototype, respectively (Fig. 1). The waterproof membrane was placed on both sides of the slope that contacted the model container to prevent water flow along the interfaces between the container and the slope. Fig. 1 shows the positions and lengths of the vertical and oblique cracks in the slope, respectively.

2.4. Measurements

An image-record and displacement measurement system was used to record the images of slope during centrifuge model tests and to measure the displacement vectors of the soil without disturbing the soil (Zhang et al., 2009). Some white granite particles were embedded onto the lateral side of the slope to increase the contrast of the image for effective measurement (Fig. 2). The displacement history of an arbitrary point on the lateral side of the soil can be measured with a sub-pixel accuracy of 0.03 mm based on the model dimensions. A rectangular Cartesian coordinate system with the origin at the top of the crack was set up to describe the positions of measurement points (Fig. 1). It is specified as positive if the position is left in the horizontal direction (x-axis) and downward in the vertical direction (y-axis). Accordingly, the displacement is positive if it is left and downward in the horizontal and vertical directions, respectively.

According to the law of similitude, the lengths of the slope and crack, the measured displacement, and the rainfall amount can be converted to the magnitudes of the prototype by multiplying by the g-level, 50. The prototype model rain intensity ratio and prototype model time ratio can be used as $1/n$ and n^2 at "n" g-level, though further investigation should be conducted on the time scale for the cohesive slope under rainfall conditions (Zhang et al., 2011). Thus, the prototype rainfall intensity ranged from 1.2 mm/hr to 3 mm/hr in the centrifuge model tests. In this paper, the lengths of the slope and crack, the measured displacement, and the rainfall amount are all presented at model dimensions.

The miniature UMS T5 tensiometers were used to measure soil suction during the tests. The tensiometer could measure a range of 0–85 kPa with an accuracy of 0.5 kPa. They were buried horizontally in the middle of the slope, and the locations are outlined in Fig. 1.

2.5. Process

In the centrifuge model test, the centrifugal acceleration was gradually increased to 50 g at first. After the displacement of the slope became stable at the 50 g-level (approximately 20 min), the rainfall or the concentrated infiltration was started. The rainfall was stopped once a significant failure (i.e., a fully initiated slide) of the slope appeared or the rainfall amount reached significant magnitude (e.g., 35–40 mm). The rainfall intensities and total rainfall amounts at failure are summarized in Table 1.

3. Infiltration analysis

A type of strain analysis was employed to analyze the deformation behavior during rainfall. The strain analysis used an isoparametric square element with four nodes, and the side length was 10 mm. The displacement vectors of these nodes were directly obtained using the image-based measurement, and the strain was accordingly computed using the fundamental scheme of the finite element method. The horizontal and vertical strains are denoted as positive if compressive.

The measured suction from a tensiometer was compared with the corresponding horizontal strain of the slope with a vertical crack (Fig. 3). It was observed that a sudden increase in strain and decrease in suction of the slope occurred simultaneously during rainfall. The suction began to decrease after a rainfall amount of 10 mm, and the strain increased significantly at that time. The increase rates of the strain and the suction also decreased at the same time. This observation was also confirmed by other tests of the slope with cracks. Similar conclusions have been obtained from the rainfall tests of different slopes in the previous studies (Wang et al., 2010b; Zhang et al., 2011). The evident decrease of soil suction indicated that the rainfall infiltrated to the measurement point of the slope; thus, the significant increase of strain was inferred to be induced by the rainfall infiltration that caused the soil softening. In other words, the moment when the strain rapidly increases means that the water from rainfall reaches the concerned point. This demonstrated that the strain history of the slope, which can be obtained using image measurement, provided an effective method to determine the infiltration field of the slope in alternative of the suction measurement because the suctions of only a few points can be measured with the buried tensiometers. The infiltration field in a slope can be described using the wetting front, which is defined as the boundary that the water infiltrates into the slope at a specific amount of rainfall. Thus, the wetting front can be yielded by connecting the points where the strain began to increase significantly at a given rainfall amount according to the strain analysis of the slope. It should be noted that such a determination method of the wetting front can be valid under conditions where only rainfall was applied on the cohesive slope, that is, there was no other load on the slope that can induce the deformation of the slope (e.g., the series of tests in this paper).

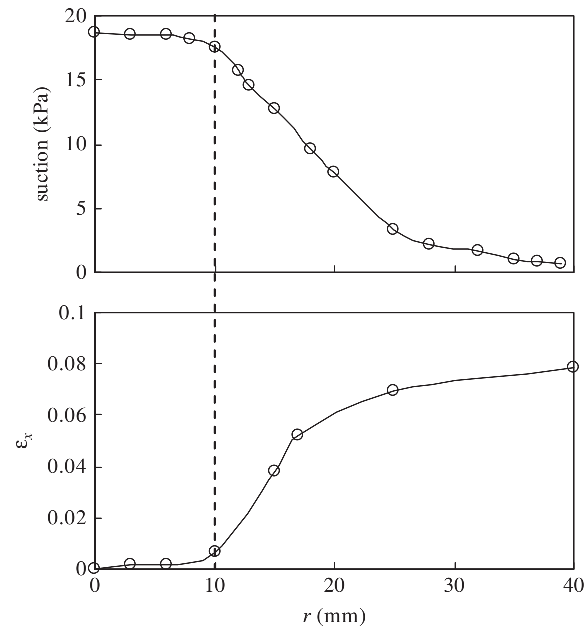

Fig. 3. Histories of horizontal strain and suction at #1 tensiometer's position in 2# tests. ε_x, horizontal strain; r, rainfall amount.

Fig. 4 shows the wetting fronts at different rainfall amounts of the slope with a vertical crack in a rainfall test. It should be noted that the strain of the slope close to the crack could not be accurately measured; thus the wetting front was broken near the crack. It was shown that the wetting front moved into the slope with increasing rainfall amount. The wetting front of the slope curved significantly near the vertical crack, demonstrating that the vertical crack induced deeper infiltration around it. This was different from the shape of the wetting front near the slope top of the homogenous slope, which was approximately parallel to the slope surface (e.g., Zhang et al., 2011), whereas the wetting front was nearly parallel with the slope surface further from the crack, similar to that of the homogeneous slope. It can be concluded that the crack caused rainfall to infiltrate faster and deeper into the slope near the location of the crack, and its influence on the

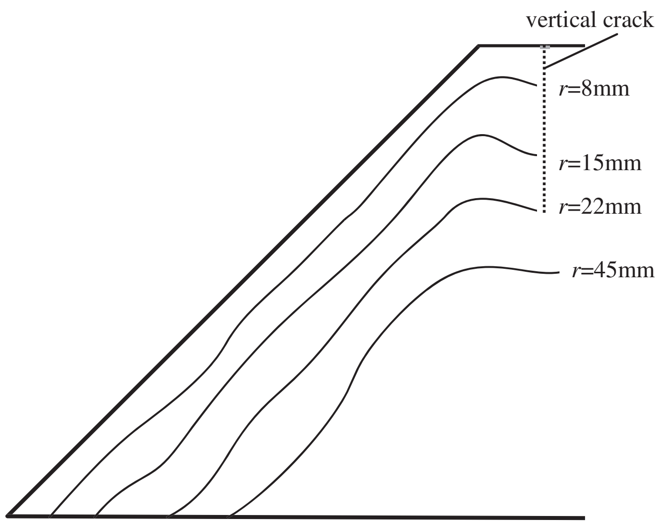

Fig. 4. Development of wetting fronts of the slope with a vertical crack (3♯ test). r, rainfall amount.

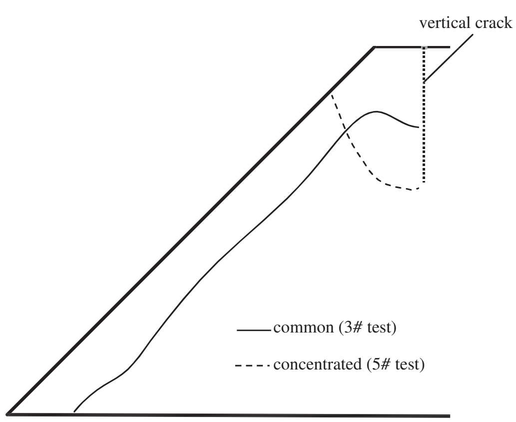

Fig. 5. Wetting fronts corresponding to different infiltration styles at a rainfall amount of 15 mm.

infiltration decreased with increasing distance from the crack.

Fig. 5 compares the wetting fronts of the slope with a vertical crack under rainfall conditions and concentrated infiltration conditions. It should be noted that the amount of infiltration water was converted to the equivalent rainfall amount for a visual and simplified comparison with the assumption that the amounts of water under the two types of rainfalls that reached the entire slope were the same. The rainfall style was demonstrated to have a significant effect on the wetting front. The concentrated infiltration induced a wetting front around the crack, which differed significantly from the wetting front induced by the rainfall condition. This implied that the wetting front of the slope was mainly dependent on the location and geometric features of the crack under the concentrated infiltration condition. Thus, concentrated infiltration focuses the study upon the effect of the crack on the infiltration behavior and successive deformation–failure behavior of the slope.

4. Deformation analysis

4.1. Displacement response

Fig. 6 shows the vectors of displacement of a slope with a vertical crack at different rainfall amounts according to the image-based measurements. It can be concluded that the displacement of the slope increased with increasing rainfall amount and decreased from the surface to the interior of the slope as a whole. The deformation was mainly concentrated near the surface of the slope, and it was concluded to be mainly dependent on the rainfall infiltration. In other words, the deformation behavior of the slope had a close relationship with the infiltration behavior.

Fig. 7 shows the histories of the vertical displacement of two typical points of a slope with a vertical crack during rainfall. The increase rate, which was defined as the ratio of vertical displacement increment versus rainfall amount increment, $\Delta v/\Delta r$, was also illustrated in the figure. While the vertical displacement of the slope increased gradually as the rainfall amount increased, the increase rate varied in different stages. For the point near the slope surface

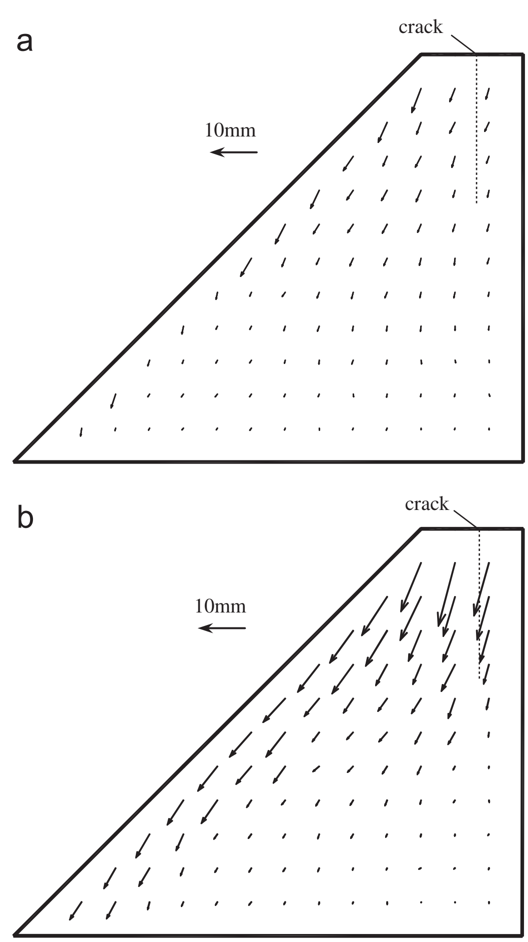

Fig. 6. Displacement vectors of the slope with a vertical crack at different rainfall amounts (3♯ test). (a) rainfall amount: 10 mm and (b) rainfall amount: 30 mm.

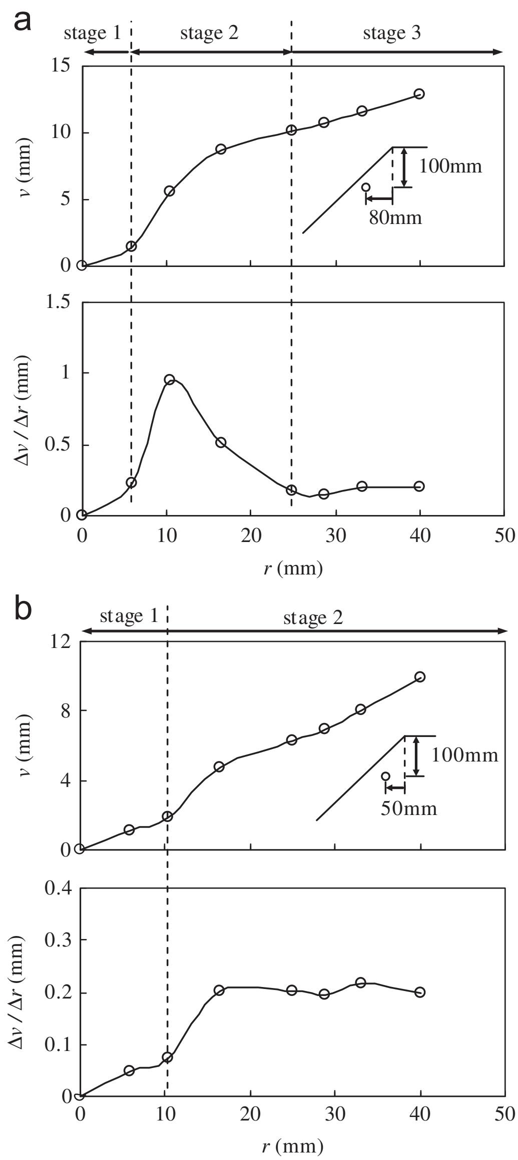

Fig. 7. Displacement histories of typical points of a slope with a vertical crack (3# test). v, vertical displacement; $\Delta v/\Delta r$, increase rate of vertical displacement; r, rainfall amount.

(Fig. 7a), the increase rate of vertical displacement was small in the first stage when the rainfall amount was less than 5 mm. As the rainfall amount increased beyond 5 mm, the increase rate of vertical displacement rose rapidly with increasing rainfall amount. This implied that the rainfall had penetrated to the soil around this point and caused the soil to soften due to an increase in water content. As the increase of vertical displacement lessened, the displacement process entered the third stage. It is noted that the rate exhibited a small fluctuation after the peak, which was mainly induced by the measurement errors of the displacement. Accordingly, the displacement exhibited a slow increase after the rainfall amount reached 24 mm, thus showing that the rainfall infiltration had a small effect on the deformation of this point. Thus, the displacement process of the slope can be generally divided into: (1) the small displacement stage, (2) the rapid increase stage, and (3) the stable stage. It should be noted that similar stage divisions have been illustrated on the homogenous slope (Zhang et al., 2011). Thus, the rainfall-induced deformation mechanism of the slope, which was derived from the homogeneous slope (Zhang et al., 2011), can also be applied to a slope with cracks. The deformation of the slope was mainly caused by the saturation of the soil and the crack-affected water infiltration under rainfall conditions.

For the point in the interior of the slope (e.g., Fig. 7b), the displacement entered the second stage later (at approximately 10 mm of rainfall amount) compared with the point near the slope surface. In addition, the third stage did not occur when the test ceased at the point, demonstrating that the soil had not yet become saturated around the point.

4.2. Effect of cracks

Closer examination was conducted on the horizontal distribution of the vertical displacement of the slopes with vertical cracks, and the measured results of the homogeneous slope are also presented for a comparison (Fig. 8). The results clearly indicated that the vertical displacement of the homogeneous slope decreased with increasing distance from the slope surface at an elevation. However, the vertical displacement of the slope with a crack exhibited a different feature in the horizontal distribution near the crack. At $y=30$ mm and $y=80$ mm, the vertical displacement of the slope with a vertical crack increased with decreasing distance from the crack, and the increased gradient became evident near the crack. In addition, the vertical displacement of the slope with a crack was significantly greater than that of the homogeneous slope near the crack. The difference in the displacement between the slopes with and without cracks weakened with increasing distance from the crack and can thus be ignored near the slope surface. For instance, the displacement of the slope with a crack was nearly equivalent to that of the homogeneous slope at $y=150$ mm, that is, further from the crack. This demonstrated that the crack had a significant effect on the deformation of the slope near the crack, inferring that the deformation was induced by the rainfall infiltration due to the crack. The boundary of the crack-influence zone can be outlined by the bifurcation points of the horizontal distribution curves of displacement between the slopes with and without cracks (Fig. 8). The crack-influence zone can be used to describe the effect of the crack on the deformation of the slope, which was found to be widest near the crack bottom.

The displacement vectors of the slope turned toward the vertical direction near the crack, while they were nearly parallel to the slope surface when further from the crack (Fig. 6). This demonstrated that the vertical displacement was significantly greater than the horizontal displacement near the crack, while the vertical displacement was similar to the horizontal displacement at the specific point that was slightly farther from the crack. Additional comparisons were conducted to compare the strain

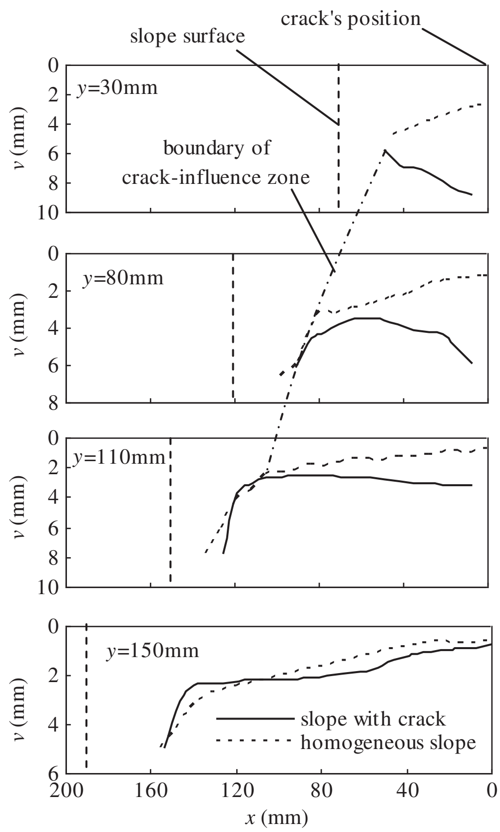

Fig. 8. Horizontal distributions of vertical displacement of homogeneous slope and of a slope with a vertical crack (3♯ test) at a rainfall amount of 20 mm. v, vertical displacement; x, horizontal coordinate; y, vertical coordinate.

histories of the two typical elements that were near and far from the crack, respectively (Fig. 9). It was shown that both the horizontal and vertical strains increased as the rainfall amount increased. The vertical strains of the slope near the vertical crack were significantly larger than the horizontal strains (Fig. 9a), while the difference between the horizontal and vertical strains was relatively small if the observation element was far from the crack (Fig. 9b). It can be concluded that significant vertical deformation was induced near the vertical crack due to the significant infiltration at that location.

Fig. 10 compares the horizontal distribution of the vertical displacement of the slope with a vertical crack corresponding to different rainfall styles, namely common rainfall and concentrated infiltration. It is evident that the displacement of the slope exhibited peak values at the crack for both rainfall styles; however, its magnitude was significantly affected by the rainfall styles. The concentrated infiltration style induced greater displacement than the common rainfall style because the former rainfall style caused more significant infiltration over the slope and led to larger deformation than the latter.

Fig. 11 compares the vertical displacement distribution along a horizontal line of the slope with vertical and oblique cracks. The vertical displacement decreased from the surface to the interior of the slope with the oblique crack, and it exhibited a maximum near the crack if the crack was vertical. This indicated that the oblique crack can yield a different displacement distribution of the slope compared with the vertical crack. The oblique crack induced a larger displacement of the slope than the vertical crack near the slope surface (left-most part of the curve) because the oblique crack was closer to the slope surface. It can be inferred that the direction of the crack significantly affected the deformation of the slope.

5. Failure analysis

An evident slip surface occurred in the slope with an oblique crack in 4♯ test (Fig. 12). A block of soil in the upper slope slid down along the oblique crack and deposited at the toe of the slope. Two tensile cracks also appeared in the top of the slope. A couple of points located on different sides and 5 mm from the crack (e.g., the slip surface of the slope) were selected to measure their relative displacement. Fig. 13 shows the histories of the relative displacement at two adjacent points 5 mm from each side of the crack, 70 mm below the top of the slope, and tangential and normal to the slip surface. It is evident that the tangential relative displacement of the point couple increased with increasing rainfall amount and exhibited an evident inflexion, while the normal relative displacement was fairly small during the test. This demonstrated that a significant slippage occurred along the oblique crack and eventually developed into a slip surface.

The slope with a vertical crack exhibited a different response under rainfall conditions (Fig. 14). For example, there was no evident slide in the slope. Few cracks appeared in the top of the slope when concentrated infiltration was applied, and only surface erosion occurred under common rainfall conditions. This demonstrated that the vertical crack, in contrast to the oblique crack, did not result in global landslide under rainfall conditions, though evident deformation was induced if the crack was located on the slope top. The reason that a full landslide is not generally formed from the vertical crack is most likely due to the position of the crack and the features of the deformation distribution. For example, compared with the vertical crack, the oblique crack was closer to the slope surface, which means that the slip surface is more likely to appear along the crack and extend to the slope surface. Therefore, it can be concluded that the inclination of the crack had a significant effect on the failure behavior of the slope under rainfall conditions.

Furthermore, rain intensity was found to affect the deformation–failure behavior of the slope with cracks. For example, according to the observations of the slopes with a vertical crack under the same rainfall amount, the slope surface was significantly washed out if the rain intensity was comparatively large (e.g., 1♯ test), while the slope mainly exhibited notable deformation if the rain intensity was relatively small (e.g., 3♯ test). It should be noted that

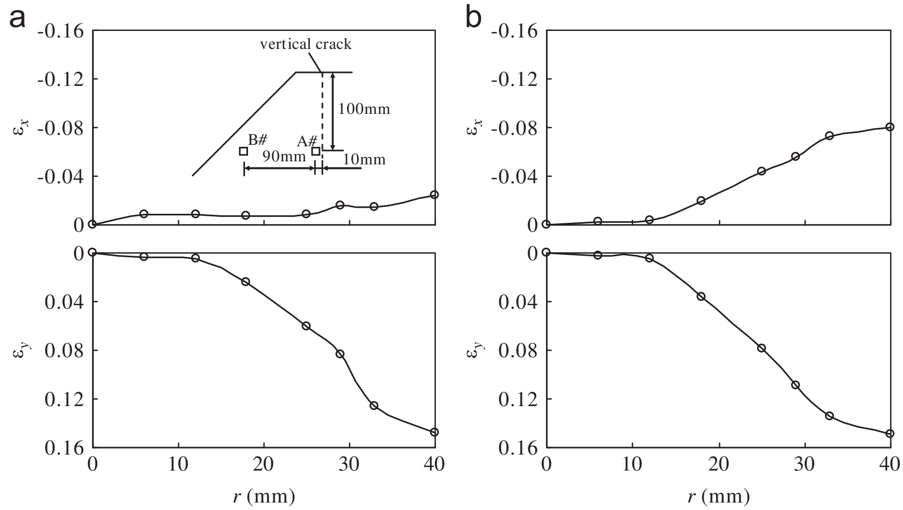

Fig. 9. Strain histories of typical points of the slope with a vertical crack (3# test). ε_x, horizontal strain; ε_y, vertical strain; r, rainfall amount. (a) element A# and (b) element B#.

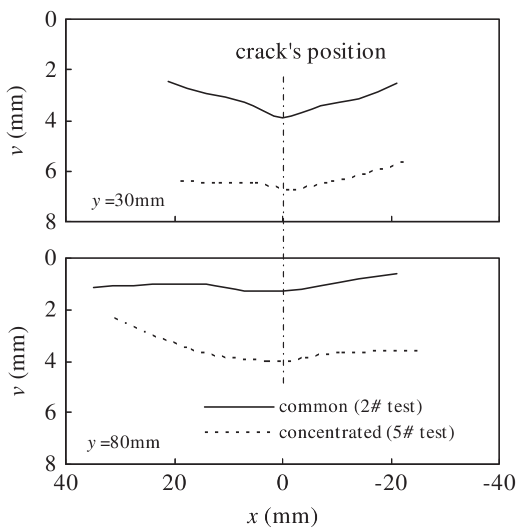

Fig. 10. Horizontal distributions of the vertical displacement of the slope with a vertical crack using different rainfall styles at an equivalent rainfall amount of 5 mm. v, vertical displacement; x, horizontal coordinate; y, vertical coordinate.

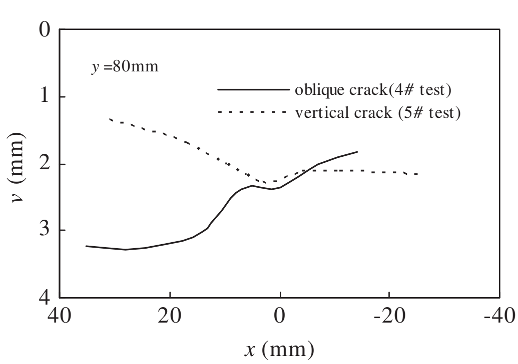

Fig. 11. Horizontal distribution of the vertical displacement of slopes with vertical and oblique cracks at a concentrated infiltration amount of 0.35 L. v, vertical displacement; x, horizontal coordinate; y, vertical coordinate.

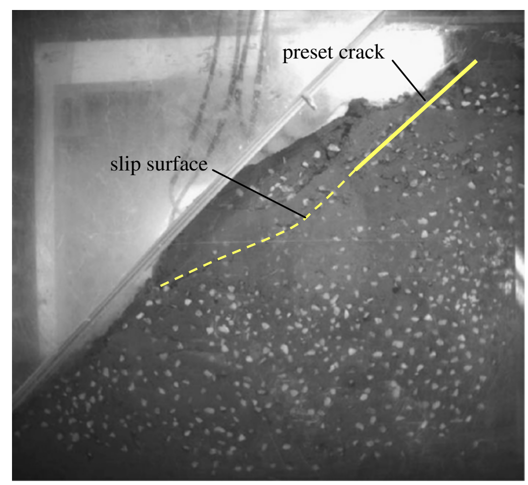

Fig. 12. Final failure of the slope with an oblique crack (4# test).

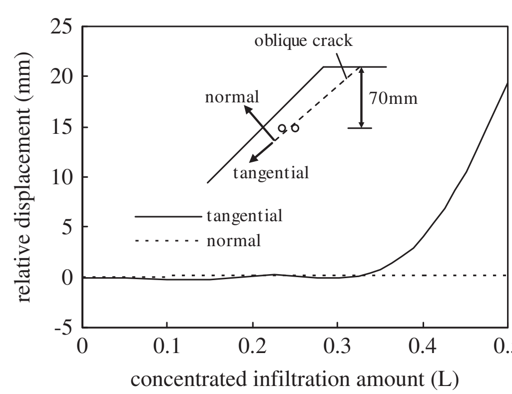

Fig. 13. Relative displacement history of a point couple along crack of the slope with an oblique crack (4# test). The horizontal distance between the measurement points and the crack was 5 mm.

systematic tests are needed in the future study to discover the influence of the rainfall intensity on the behavior of the slopes.

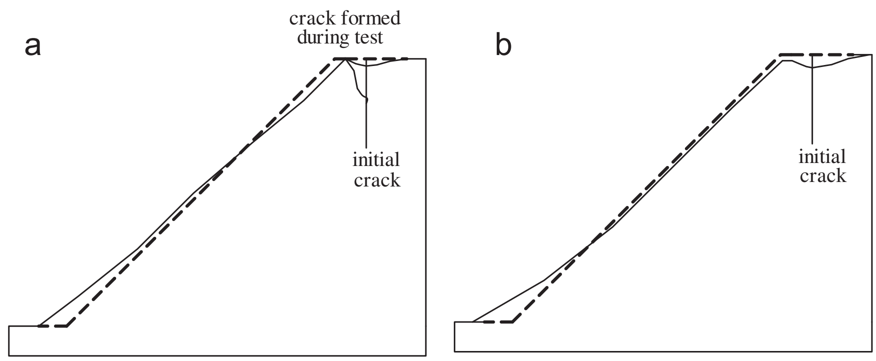

Fig. 14. Final failure of the slope with vertical cracks. (a) concentrated infiltration (5# test) and (b) common rainfall(2# test).

6. Conclusions

A series of centrifuge model tests was conducted on slopes with different types of cracks under rainfall conditions. The main conclusions were drawn by analyzing the measurement results of the observations as follows:

(1) The features of the crack, such as the inclination, had a significant effect on the water infiltration within the slope under rainfall conditions. For example, the wetting front curved notably near the vertical crack.
(2) The deformation of the slope was mainly caused by the saturation of the soil under rainfall conditions, which was affected by the crack through its effect on the water infiltration. The displacement process of the slope with cracks can be divided into the small displacement stage, the rapid increase stage, and the stable stage.
(3) The extent of the influence of the crack on the infiltration and deformation of the slope decreased as the distance from the crack increased. This phenomenon can be described using the crack-influence zone with the greatest width near the crack bottom.
(4) Rainfall induced the significant vertical deformation near the vertical crack rather than the horizontal deformation of the slope.
(5) In comparison with the oblique crack, the vertical crack was unlikely to lead to global landslide under rainfall conditions if the cracks were located on the slope top.
(6) The deformation–failure behavior of the slope with cracks was affected by both rainfall style and rain intensity.

Acknowledgments

The study is supported by Key Laboratory of Geotechnical and Underground Engineering of Ministry of Education, Tongji University (No. KLE-TJGE-B0901); and National Natural Science Foundation of China (Nos. 51079073, 50979045).

References

Anderson, M.G., Pope, R.G., 1984. The incorporation of soil water physics models in geotechnical studies of landslide behavior.In: Proceedings of the 4th International Symposium on Landslides, vol. 4, pp. 349–354.

Fan, P., Liu, Q.Q., Li, J.C., Sun, J.P., 2005. Numerical analysis of rainfall infiltration in the slope with a fracture. Science in China 48(S), 107–120.

Hu, S., (2000). Reliability of slope stability considering infiltration through surface cracks. M.Phil. Thesis, Hong Kong University of Science and Technology.

Hudacsek, P., Bransby, M.F., Hallett, P.D., Bengough, A.G., 2009. Centrifuge Modelling of Climatic Effects on Clay Embankments. Proceedings of the Institution of Civil Engineers-Engineering Sustainability 162 (2), 91–100.

Iverson, R.M., 2000. Landslide triggering by rain infiltration. Water Resources Research 36 (7), 1897–1910.

Kimura, T., Takemura, J., Sucmasa, N., Hiro-oka, A., (1991). Failure of fills due to rain fall. In: Proceedings of the International Conference Centrifuge, 1991, pp. 509–516.

Lim, T.T., Rahardjo, H., Chang, M.F., Fredlund, D.G., 1996. Effect of rainfall on matric suction in a residual soil slopes. Canadian Geotechnical Journal 33 (2), 618–628.

Montrasio, L., Valentino, R., Losi, G.L., 2009. Rainfall-induced shallow landslides: a model for the triggering mechanism of some case studies in northern Italy. Landslides 6 (3), 241–251.

Moriwaki, H., Inokuchi, T., Sassa, K., Ochiai, H., Wang, G., 2004. Failure process in a full-scale landslide experiment using a rainfall simulator. Landslides 1 (4), 277–288.

Rogers N.W., Selby M.J. (1980). Mechanisms of Shallow Translational Landsliding during Summer Rainstorms: North Island, New Zealand, Geografiska Annaler Series A, Physical Geography, 62(1/2), pp. 11–21.

Take, W.A., Bolton, M.D., Wong, P.C.P., Yeung, F.J., 2004. Evaluation of landslide triggering mechanisms in model fill slopes. Landslides 1 (3), 173–184.

Tohari, A., Nishigaki, M., Komatsu, M., 2007. Laboratory rainfall-induced slope failure with moisture content measurement. Journal of Geotechnical and Geoenvironmental Engineering 133 (5), 575–587.

Trandafir, A.C., Sidle, R.C., Gomi, T., Kamai, T., 2008. Monitored and simulated variations in matric suction during rainfall in a residual soil slope. Environmental Geology 55 (5), 951–961.

Viswanadham, B.V.S., Rajesh, S., 2009. Centrifuge model tests on clay based engineered barriers subjected to differential settlements. Applied Clay Science 42 (3–4), 460–472.

Wang, L.P., Zhang, G., Zhang, J.M., 2010a. Nail reinforcement mechanism of cohesive soil slopes under earthquake conditions. Soils and Foundations 50 (4), 459–469.

Wang, R., Zhang, G., Zhang, J.M., 2010b. Centrifuge modelling of clay slope with montmorillonite weak layer under rainfall conditions. Applied Clay Science 50 (3), 386–394.

Wang, G., Sassa, K., 2001. Factors affecting rainfall-induced flowslides in laboratory flume tests. Geotechnique 51 (7), 587–599.

Yuki, M., Tsuyoshi, H., Yukinori, M., 2006. Mechanisms of shallow landslides on soil-mantled hillslopes with permeable and impermeable bedrocks in the Boso Peninsula, Japan. Geomorphology 76, 92–108.

Zhang, G., Hu, Y., Zhang, J.M., 2009. New image analysis-based displacement–measurement system for geotechnical centrifuge modeling tests. Measurement 42 (1), 87–96.

Zhang, G., Qian, J.Y., Wang, R., Zhang, J.M., 2011. Centrifuge model test study of rainfall-induced deformation of cohesive soil slopes. Soils and Foundations 51 (2), 297–305.

Zolfaghari, A.R., Andrew, C.H., Paul, F.M., 2005. Simple genetic algorithm search for critical non-circular failure surface in slope stability analysis. Computers and Geotechnics 32, 139–152.